International Conference on Computational Methods in Marine Engineering
MARINE 2011
L.Eça, E. Oñate, J. García, T. Kvamsdal and P. Bergan (Eds)

ADVANCES IN THE DEVELOPMENT OF A TIME-DOMAIN UNSTRUCTURED FINITE ELEMENT METHOD FOR THE ANALYSIS OF WAVES AND FLOATING STRUCTURES INTERACTION

MARINE 2011

BORJA SERVAN-CAMAS*, JULIO GARCIA-ESPINOSA*

*International Center for Numerical Methods in Engineering (CIMNE)
Universidad Politécnica de Cataluña
Campus Norte UPC, 08034 Barcelona, Spain
e-mail: bservan@cimne.upc.edu, julio@cimne.upc.edu
web page: http://www.cimne.com

Key words: wave structure interaction; finite element; time domain; unstructured mesh.

Summary. Being capable of predicting wave-structure interaction in the time domain is of great interest for the offshore industry. However most computer programs used in the industry work in the frequency domain. Therefore, the main objective of this work is the development a time domain solver based on the finite element method capable of solving wave-structure interaction problems using unstructured meshes. We found good agreement between the numerical results we obtained and analytical solutions as well as numerical solutions obtained by other numerical method.

1 INTRODUCTION

Wave structure interaction is a topic of great interest in naval and offshore engineering. This interest is growing in the last years due to the boost given by the development of the marine renewable energy field. In this context, the development of time-domain wave structure interaction programs is a main request from the industry.

Up to date the numerical simulation of wave structure interaction has been mostly carried out using the frequency domain. The reason might be that the computational cost of time domain simulations were too high and computational time was too large. Moreover, assumptions like linear waves and the harmonic nature of water waves made the frequency domain to be the right choice. However, nowadays computing capabilities make possible to carry out numerical simulations in the time domain in a reasonable time, with the advantage of making easier the coupling with other phenomena.

Regarding the numerical method usually adopted, the boundary element method (BEM) has dominated over others like finite element method (FEM). The main advantage of BEM over FEM resides in the fact that only boundary meshes are required, while FEM demands meshing the whole volume, with the corresponding increase in the number of variables of the discrete problem. However, despite of the higher number of variables required by FEM, it is not clear that BEM has to be more efficient. Mostly due to the sparse pattern in FEM and the

large availability of iterative solver preconditioners that can improve the resolution of the corresponding linear system of equations. In [1] Cai et al. a heuristic comparison between both methods is given and demonstrate that a solution to the boundary value problem can be obtained more efficiently by the FEM.

In the last decade, there have been extensive applications of the finite element method (FEM) to free surface problems. For example, Oñate and García [2] presented a stabilized FEM for fluid structure interaction in the presence of free surface where the latter was modelled by solving a fictitious elastic problem on the moving mesh. In [3,4] Löhner et al. developed a FEM capable of tracking violent free surface flows interacting with objects. Also García et al. [5] developed a new technique to track complex free surface shapes. However, many works like the previous ones are based on solving the Navier-Stokes equations, too expensive computationally speaking when it comes to simulating many real problems regarding ocean waves interacting with floating structures, which can be more cheaply simulated using potential flow theory along with Stokes perturbation approximation.

Despite of the great effort invested in the last years to the development of FEM algorithms, to the authors' knowledge, yet there has not been developed a FEM for solving first order waves, based on Stokes perturbation, interacting with structures in the time domain using unstructured meshes. The use of structure or semi-structures meshes is a big limitation since it limits the complexity of the geometry to be used. In this study we present a FEM for wave-structure interaction that can be used with unstructured meshes. Besides, since it is based on Stokes wave theory, no re-meshing or moving mesh technique are needed, which keeps computational costs and times low. The algorithm has been adapted to include non-linear external forces, like those used to define mooring systems, and variations on the pressure over the free surface.

2 PROBLEM STATEMENT

2.1 Governing equations

We consider the first order diffraction-radiation problem of a floating body.

$$\nabla^2\varphi = 0 \text{ in } \Omega \tag{1}$$

$$\partial_t\varphi + g\eta = -P_a/\rho + C \text{ in } z = 0 \quad \text{(dynamic free surface boundary condition)} \tag{2}$$

$$\partial_t\eta - \partial_z\varphi = 0 \text{ in } z = 0 \quad \text{(kinematic free surface boundary condition)} \tag{3}$$

$$\partial_z\varphi = 0 \text{ in } z = -H \tag{4}$$

$$\nabla\varphi\cdot\mathbf{n}_B = \mathbf{v}_B\cdot\mathbf{n}_B \text{ in } \Gamma_B \tag{5}$$

where φ and η are the first order potential and free surface elevation respectively; Ω is the fluid domain bounded by $z = 0$; P_a is the atmospheric pressure; ρ is the water density; C is a constant value; Γ_B represents the wetted surface of a floating body; and H is the water depth. The domain is assumed to be infinite in the horizontal directions.

2.2 Velocity potential decomposition

The aim of this work is to simulate the dynamics of a floating body subjected to the action of waves. To do so, we will first model the environment as the sum of a number of airy waves. This can be expressed in terms of a velocity potential given by:

$$\psi = \sum_m \frac{A_m g}{\omega_m} \frac{\cosh\left(|\mathbf{k}_m|(H+z)\right)}{\cosh\left(|\mathbf{k}_m|H\right)} \cos\left(|\mathbf{k}_m|(x\cos\alpha_m + y\sin\alpha_m - \omega_m t + \delta_m\right) \tag{6}$$

where A_m are the wave amplitudes; ω_m are the wave frequencies; $\mathbf{k}_m$ are the wave numbers; α_m are the wave directions; and δ_m are wave phases. From this point on, we will refer to ψ as the incident potential. This potential, along with the dispersion relation $\omega_m^2 = g|\mathbf{k}_m|\tanh\left(|\mathbf{k}_m|H\right)$, fulfils Eqs.(1)-(4), and therefore is solution of the mathematical model in the absence of bodies.

Let $\varphi = \psi + \phi$ be the solution to the governing equations. The equations to be fulfilled by ϕ are

$$\nabla^2\phi = 0 \quad \text{in } \Omega \tag{7}$$

$$\partial_t\phi + g\eta = -P_a/\rho + C' \text{ in } z = 0 \quad \text{(dynamic free surface boundary condition)} \tag{8}$$

$$\partial_t\eta - \partial_z\phi = 0 \text{ in } z = 0 \quad \text{(kinematic free surface boundary condition)} \tag{9}$$

$$\partial_z\phi = 0 \quad \text{in } z = -H \tag{10}$$

$$\nabla\phi\cdot\mathbf{n}_B = \left(\mathbf{v}_B - \nabla\psi\right)\cdot\mathbf{n}_B \quad \text{in } \Gamma_B \tag{11}$$

3.1 Radiation condition and wave absorption

We will make use of a Sommerfeld radiation condition at the edge of the computational domain: $\partial_t\phi + c\nabla\phi\cdot\mathbf{n}_R = 0$ in the surface limiting of the domain in the horizontal directions, and c is a prescribed wave velocity. Wave dissipation is also introduced into the dynamic free surface boundary condition by varying the pressure such that $P_a/\rho = P_0 + \kappa(\mathbf{x})\partial_z\phi$ where $\kappa(\mathbf{x})$ is a damping coefficient. Combining the dynamic and kinematic boundary condition, introducing the wave absorption and choosing $C' = P_0$, the governing equations for ϕ becomes:

$$\nabla^2\phi = 0 \quad \text{in } \Omega \tag{12}$$

$$\partial_{tt}\phi = -g\partial_z\phi - \kappa(\mathbf{x})\partial_t\partial_z\phi \text{ in } z = 0 \tag{13}$$

$$\partial_z\phi = 0 \quad \text{in } z = -H \tag{14}$$

$$\nabla\phi\cdot\mathbf{n}_B = \left(\mathbf{v}_B - \nabla\psi\right)\cdot\mathbf{n}_B \quad \text{in } \Gamma_B \tag{15}$$

$$\partial_t\phi + c\nabla\phi\cdot\mathbf{n}_R = 0 \quad \text{in } \Gamma_R \tag{16}$$

$$\eta = -\frac{1}{g}\partial_t\phi - \frac{P_a}{\rho g} + \frac{C'}{g} \text{ in } z = 0 \quad \text{(kinematic free surface boundary condition)} \tag{17}$$

3 FINITE ELEMENT FORMULATION

The discrete variational problem:

$$\int_{\Omega} \nabla v_h \cdot \nabla \phi_h d\Omega = \int_{\Gamma^B} v_h \cdot \hat{\phi}_n^B d\Gamma + \int_{\Gamma^R} v_h \cdot \hat{\phi}_n^R d\Gamma + \int_{\Gamma^{Z_0}} v_h \cdot \hat{\phi}_n^{Z_0} d\Gamma + \int_{\Gamma^{Z_{-H}}} v_h \cdot \hat{\phi}_n^{Z_{-H}} d\Gamma \quad \forall v_h \in Q_h \quad (18)$$

where $\hat{\phi}_n^B$, $\hat{\phi}_n^R$, $\hat{\phi}_n^{Z_0}$ and $\hat{\phi}_n^{Z_{-H}}$ are the potential normal gradients corresponding to the Neumann boundary conditions on body, radiation boundary, free surface and bottom, respectively. The associated matrix form is:

$$\overline{\overline{\mathbf{L}}}\boldsymbol{\phi} = \mathbf{b}^B + \mathbf{b}^R + \mathbf{b}^{Z_0} + \mathbf{b}^{Z_{-H}} \quad (19)$$

3.1 Boundary conditions

The right hand side of Eq. (19) is implemented as follows:

$$\begin{aligned}(\mathbf{b}^{Z_0})^{n+1} = &-\overline{\overline{\mathbf{M}}}_{\Gamma^{Z_0}} \left(\frac{12}{g\Delta t^2 + 6\kappa(\mathbf{x})\Delta t} (\boldsymbol{\phi}^{n+1} - 2\boldsymbol{\phi}^n + \boldsymbol{\phi}^{n-1}) \right) \\ &- \overline{\overline{\mathbf{M}}}_{\Gamma^{Z_0}} \left(\frac{10 g\Delta t}{g\Delta t + 6\kappa(\mathbf{x})} (\boldsymbol{\phi}_z^{Z_0})^n + \left(\frac{g\Delta t - 6\kappa(\mathbf{x})}{g\Delta t + 6\kappa(\mathbf{x})} \right) (\boldsymbol{\phi}_z^{Z_0})^{n-1} \right)\end{aligned} \quad (20)$$

$$\left(\mathbf{b}^R\right)^{n+1} = \overline{\overline{\mathbf{M}}}_{\Gamma^R} \left(\boldsymbol{\phi}_n^R\right)^{n+1} = \frac{1}{\Delta t} \overline{\overline{\mathbf{M}}}_{\Gamma^R} \left(\boldsymbol{\phi}^n - \boldsymbol{\phi}^{n-1}\right) \quad (21)$$

$$\left(\mathbf{b}^B\right)^{n+1} = \overline{\overline{\mathbf{M}}}_{\Gamma^B} \left(\boldsymbol{\phi}_n^B\right)^{n+1} \quad (22)$$

The free surface and pressure are computed by the following fourth order finite difference scheme:

$$\eta^{n+1} = -\frac{1}{g\Delta t} \left(\frac{25}{12}\varphi^{n+1} - 4\varphi^n + 3\varphi^{n-1} - \frac{4}{3}\varphi^{n-2} + \frac{1}{4}\varphi^{n-3} \right) \quad (23)$$

$$P^{n+1} = -\rho g z - \frac{\rho}{\Delta t} \left(\frac{25}{12}\varphi^{n+1} - 4\varphi^n + 3\varphi^{n-1} - \frac{4}{3}\varphi^{n-2} + \frac{1}{4}\varphi^{n-3} \right) \quad (24)$$

3.2 Body dynamics

Integrating the pressure over the body surface, the resulting forces and moments are obtained. On the other hand, the body dynamics is given by the equation of motion:

$$\overline{\overline{M}}\mathbf{X}_{tt} + \overline{\overline{K}}\mathbf{X} = \mathbf{F} \quad (25)$$

where $\overline{\overline{M}}$ is the mass matrix; $\overline{\overline{K}}$ is the hydrostatic restoring coefficient matrix; $\mathbf{F}$ is the hydrodynamic forces induced over the body plus any other external forces; and $\mathbf{X}$ represent the movement of the six degrees of freedom. we use a implicit Newmark´s average acceleration method to carry out the temporal integration of Eq. (25)

3.3 Free surface boundary condition for OWC calculations

In order to be able to simulate OWC devices, a non-linear free surface boundary condition has been developed based on the characteristic curves of the Wells-turbines type used in these devices. For instance, based on the manufacturer information and working in ideal conditions, the Wavegen 18.5Kw turbine get a power output and pressure that relates to the flux as:

$$p(q) = 0.0779|q|^3 - 0.065q^2 + 0.1933|q| \tag{26}$$

$$P(q) = 164.07 \cdot q \cdot |q| \tag{27}$$

where p is the output power in kilowatts, P is the pressure drop across the turbine in Pascals, and q is the instantaneous air flux flowing through the turbine in cubic meters per second. The pressure obtained by eq. (27) is introduced into the dynamic condition of the free surface as

$$\frac{\phi^{n+1} - 2\phi^n + \phi^{n-1}}{\Delta t^2} = -\frac{1}{12} g\left(\partial_z \phi^{n+1} + 10\partial_z \phi^n + \partial_z \phi^{n-1}\right) - \frac{1}{12\rho}\left(\partial_t P^{n+1} + 10\partial_t P^n + \partial_t P^{n-1}\right) \tag{28}$$

$$\partial_t P^{n+1} \simeq \left(3P^{n+1} - 4P^n + P^{n-1}\right)/\left(2\Delta t\right) \tag{29}$$

4 NUMERICAL RESULTS

4.1 Waves refracted by a vertical circular cylinder

In this section we solve the problem of a monochromatic wave interacting with a fix bottom mounted circular cylinder. The analytical solution for the incident and scattered waves can be found in [6]. Next we compare numerical results obtained by the analytical solution with numerical results obtained by our FEM schemes for the specific case of $R = 1$, $H = 1$, $A = 0.1$, $L = 2$. Using $g = 9.81$ and by mean of the dispersion relation for first order waves, we obtain the frequency value $\omega = \sqrt{g\pi \tanh(\pi)} = 5.5411\,\text{rad/s}$, and the wave period T = 1.1339s. Figure 1 left compares the contour lines of the free surface elevation at any time $t = nT$. It can be observed that the FEM solution mostly lie over the analytical solution. . Figure 1 center compares the pressure distribution over the cylinder obtained by the analytical solution and the FEM solution. Both pressure distributions are obtained using the same colour scale, with a maximum value of 1500 and a minimum of 2000. Figure 1 right compares the force induced over the cylinder obtained by the analytical solution and FEM. It can be seen that the forces obtained in both ways are quite close to each other.

4.2 Freely floating circular cylinder

In this section we analyze the seakeeping behaviour of a freely floating cylinder subject to the action of monochromatic waves. The cylinder parameters are; Radius=1m; draft=0.5m; xg=0; yg=0; zg=0; Ixx/Mass=1; Iyy/Mass=1; Izz/Mass=1.Simulations were carried out for periods ranging between half a second and five seconds. Figure 2 compares the response amplitude operators (RAOs) obtained by the present FEM model and RAOs obtained by the well known program WAMIT, which is based on the BEM. Both results agree well and only some small differences are observed in the resonance area for the pitch movement, probably due to the different numerical dissipation added in that case in the BEM and FEM

formulations.

4.3 Oscillating water column test

In this section, the FEM model was used to analyze the performance of an OWC device to absorb energy from waves. The OWC consist of a circular bell of 5 meters in diameter (inner), 0.5 meters in thickness, and 2.5 meter in draft. The water depth is 20 meters and the OWC device will be subject to the action of monochromatic waves with periods ranging between 3 and 5 seconds. The free surface elevation was analyzed within the chamber in the absence of the turbine (P=0). Figure 3 shows response amplitude operators obtained as $\xi = Q_{\max} /(A\pi R^2 \omega)$, where $Q_{\max}$ is the instantaneous flux amplitude; A is the wave amplitude; R is the inner radius of the OWC device; ω is the wave frequency; and ξ represents the average amplitude of the free surface elevation within the device.

The performance of the same OWC device was also analyzed after installing a Wells-type turbine, the Wavegen 18.5Kw model. The imposition of Eq. (26) implies that the problem is no linear anymore. Therefore, the performance of the system was analyzed for three wave amplitudes and a range of periods.

Table 1 summarizes the results obtained from the simulation, where the columns named power provide the average power supplied by the device, and the efficiency is obtained from dividing the average power by the power transported by a wave front of 5 meters.

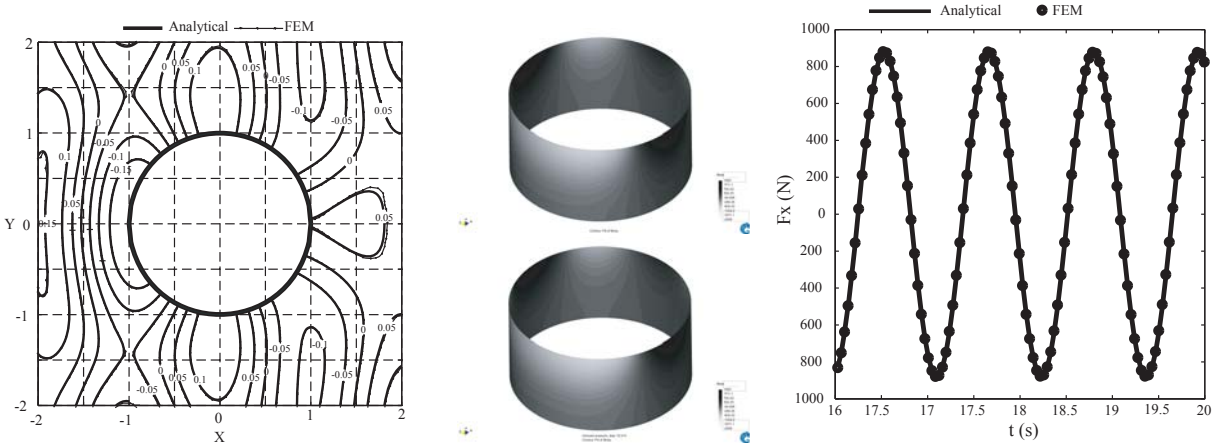

Figure 1: Left**:** Contour lines of free surface elevation at $t = nT$. Comparison between analytical (solid line) and FEM (dot line) results. Center: Pressure induced on the cylinder by the velocity potential at time $t = nT$. Comparison between analytical (up) and FEM (down) results. Right: Horizontal force induced over the cylinder. Comparison between analytical (solid line) and FEM (dots) results.

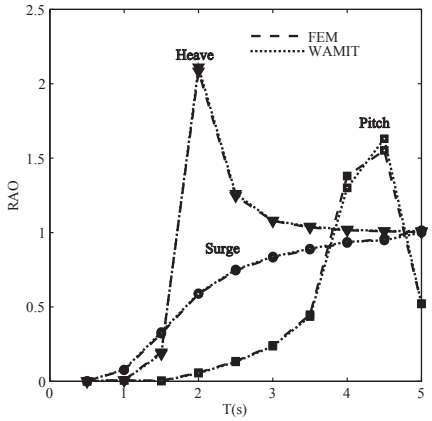

Figure 2 Response amplitude operator for freely floating cylinder. Circles (surge); triangles (heave); squares (pitch).

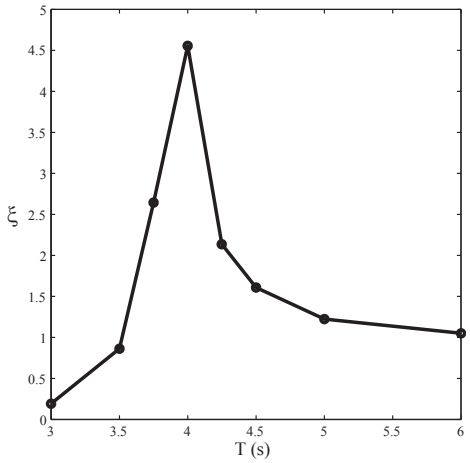

Figure 3: Response amplitude operator for oscillating water column.

	A=0.1m		A=0.5m		A=1m	
T(s)	Power (kw)	Efficiency	Power (kw)	Efficiency	Power (kw)	Efficiency
3	0,079	13,38%	0,379	2,58%	0,923	1,57%
3.5	0,150	21,85%	0,762	4,44%	1,936	2,82%
4	0,203	25,87%	1,189	6,06%	3,135	3,99%
4.5	0,234	26,44%	1,587	7,17%	4,310	4,87%
5	0,254	25,65%	2,002	8,09%	5,590	5,64%
6	0,259	21,00%	2,654	8,62%	7,790	6,32%
7	0,242	15,97%	3,082	8,14%	9,483	6,26%

Table 1: Oscillating water column results

5. Conclusions

A FEM solver for wave structure interaction in the time domain has been presented. The wave modelling is based on Stokes perturbation theory, which allows keeping the same computational domain along the simulation. The FEM has been developed so unstructured meshes can be used, no matter the complexity of the structure.

Both, the free surface and outlet boundary conditions are based on implicit schemes. They have been introduced within the system matrix so that no iterations are required within the time step to reach convergence among the Laplace and boundary conditions.

FEM results have been compared to analytical results available for a circular vertical cylinder. The agreement between both solutions shows that the algorithms develop in this work perform well. Response amplitude operators for a freely floating cylinder obtained by the present FEM and BEM also compared well.

Moreover, since the present study is based on a time domain formulation, nonlinear external forces and moments acting over structures can be easily brought into the dynamics of the structure interacting with waves. Nonlinear pressure boundary conditions have been implemented to show how the algorithms can be used to evaluate wave energy converters based on oscillating water columns.

Acknowledgements

This study was partially supported by the Ministry for Science and Innovation of Spain in the AIDMAR project CTM2008-06565-C03-01. The authors are very thankful to Mr Rafael Watai for providing the numerical results from WAMIT showed in this work.

References

[1] Cai, X., Langtangen, H. P., Nielsen, B. F. & Tveito, A., A finite element method for fully nonlinear water waves. *J. Comput. Phys*. 1998; 143: 544–568.

[2] Oñate E. & García, J., A finite element method for fluid-structure interaction with surface waves using a finite calculus formulation, *Comp. Methods Appl. Mech. and Engrg.* 2001; 191: 635-660.

[3] Löhner, R., Yang, C. & Oñate, E., On the simulation of flows with violent free surface motion, *Comp. Methods Appl. Mech. Eng*. 2006; 195: 5597-5620.

[4] Löhner, R., Yang, C. & Oñate, E., On the simulation of flows with violent free surface motion and moving objects using unstructured meshes, *Comp. Methods Appl. Mech. Eng*. 2007; 53: 1315-1338.

[5] García, J., Valls A., & Oñate, E., ODDLS: A new unstructured mesh finite element method for the analysis of free
surface flow problems, *Int. J. Numer. Meth. Fluids* 2008; 76 (9): 1297-1327.

[6] R. McCamy and R. Fuchs, Wave forces on piles: a diffraction theory, *Tech. Memo No. 69, U.S. Army Corps of Engrs*. 1954.